

# SAP18 Promotes Krüppel-dependent Transcriptional Repression by Enhancer-specific Histone Deacetylation<sup>\*[5]</sup>

Received for publication, August 8, 2008, and in revised form, November 18, 2008. Published, JBC Papers in Press, December 1, 2008, DOI 10.1074/jbc.M806163200

Alexey Matyash<sup>‡</sup>, Navjot Singh<sup>§</sup>, Steven D. Hanes<sup>§</sup>, Henning Urlaub<sup>¶</sup>, and Herbert Jäckle<sup>‡1</sup>

From the <sup>‡</sup>Abteilung Molekulare Entwicklungsbiologie and <sup>¶</sup>Bioanalytical Mass Spectrometry Group, Max-Planck-Institut für biophysikalische Chemie, Am Fassberg 11, 37077 Göttingen, Germany and the <sup>§</sup>Wadsworth Center, New York State Department of Health and Department of Biomedical Sciences, State University of New York, Albany, New York 12208

Body pattern formation during early embryogenesis of *Drosophila melanogaster* relies on a zygotic cascade of spatially restricted transcription factor activities. The gap gene *Krüppel* ranks at the top level of this cascade. It encodes a C2H2 zinc finger protein that interacts directly with *cis*-acting stripe enhancer elements of pair rule genes, such as *even skipped* and *hairy*, at the next level of the gene hierarchy. *Krüppel* mediates their transcriptional repression by direct association with the corepressor *Drosophila* C terminus-binding protein (dCtBP). However, for some *Krüppel* target genes, deletion of the dCtBP-binding sites does not abolish repression, implying a dCtBP-independent mode of repression. We identified *Krüppel*-binding proteins by mass spectrometry and found that SAP18 can both associate with *Krüppel* and support *Krüppel*-dependent repression. Genetic interaction studies combined with pharmacological and biochemical approaches suggest a site-specific mechanism of *Krüppel*-dependent gene silencing. The results suggest that *Krüppel* tethers the SAP18 bound histone deacetylase complex 1 at distinct enhancer elements, which causes repression via histone H3 deacetylation.

*Kr* (*Krüppel*) is an essential gene of the segmentation gene hierarchy in *Drosophila melanogaster*. It encodes a C2H2 zinc finger protein necessary for the formation of thoracic and abdominal body parts of the embryo (1–3). *Kr* is expressed in the central region of the embryo where it controls transcription of pair rule genes, such as *eve* (*even skipped*) and *h* (*hairy*) (4, 5). The *Kr* protein (*Kr*) binds to multiple specific DNA-binding sites (6, 7) within distinct *cis*-acting stripe elements of pair rule genes and provides repression in a concentration-dependent manner. In addition, *Kr* functions later in embryogenesis by acting as a key regulator of multiple developmental genes necessary for the formation of various organs (8–11). Furthermore, ectopic expression of *Kr* in imaginal eye discs interferes with their normal development by causing an *Irregular facet* gain-of-

function phenotype (12, 13). The available evidence suggests that *Kr* acts mainly as a transcriptional repressor (14–18) and is likely to control several hundred target genes (14, 19). However, the mechanism of *Kr*-dependent transcriptional repression is still not fully understood.

Initial *in vitro* studies showed that *Kr* is capable of forming concentration-dependent homodimers that interact with the basal transcriptional machinery and prevent transcription (20). Although this mechanism would explain a concentration-dependent action of *Kr*, its relevance for *in vivo* action of *Kr* has not yet been demonstrated. A second mechanism of *Kr*-dependent repression rests on multiple and overlapping DNA-binding sites for activators within the enhancer region of target genes. In this context, binding of *Kr* can compete for binding of activators and thereby prevent gene activation (21, 22). Finally, the C terminus of *Kr* contains functional binding sites for the corepressor dCtBP (22, 23) and acts as a repressor via distinct *cis*-acting enhancers such as the *eve* stripe 2. In the absence of the dCtBP-binding sites, *eve* stripe 2 expression cannot be repressed by *Kr*, and thus, the expression domain extends into the *Kr* expression domain. Conversely, overexpression of *Kr* throughout the blastoderm embryo causes repression of *eve* stripe 2 expression, whereas overexpression of mutant *Kr* lacking the dCtBP-binding sites has no such effect. Although the dCtBP-dependent repression by *Kr* is firmly established, the mechanism of this type of repression is not yet elucidated. In contrast to the *eve* stripe 2 enhancer, dCtBP does not seem to be necessary for *Kr*-dependent regulation of the *h* stripe 7 enhancer. Overexpression of *Kr* in maternal dCtBP mutant embryos still represses *h* stripe 7 expression (24), suggesting that there must be an additional and dCtBP-independent repressor function of *Kr*. To seek a factor that confers this missing repressor function on *Kr* and to elucidate the mechanism of this type of repressor action, we performed a protein-protein interaction screen to identify proteins that associate with *Kr*. We found dSAP18, a protein that is known to associate with components of the histone deacetylase complex 1 (dHDAC1)<sup>2</sup> (25). The results suggest that *Kr* participates in the site-specific deacetylation of histone 3 at the *h* stripe 7 element but not at the

<sup>\*</sup> This work was supported by funds from the Max-Planck-Gesellschaft (to H. J., H. U., and A. M.) and by American Cancer Society Grant RSG-9508506-DDC and March of Dimes Grant 1-FY07-527 (to V. N. S. and S. D. H.). The costs of publication of this article were defrayed in part by the payment of page charges. This article must therefore be hereby marked "advertisement" in accordance with 18 U.S.C. Section 1734 solely to indicate this fact.

<sup>[5]</sup> The on-line version of this article (available at <http://www.jbc.org>) contains supplemental Tables S1 and S2 and Figs. S1 and S2.

<sup>1</sup> To whom correspondence should be addressed: Am Fassberg 11, 37077 Göttingen, Germany. Tel.: 49-551-201-1482/3; Fax: 49-551-201-1755; E-mail: hjaeckle@gwdg.de.

<sup>2</sup> The abbreviations used are: HDAC, histone deacetylase; CtBP, C terminus-binding protein; ESI-MS/MS, electrospray ionization tandem mass spectrometry; HPLC, high performance liquid chromatography; HRP, horseradish peroxidase; PepSpot, peptide spot; TSA, trichostatin A; ChIP, chromatin immunoprecipitation; xChIP, cross-linked ChIP; GST, glutathione S-transferase; MALDI-TOF-MS, matrix-assisted laser desorption ionization time-of-flight mass spectrometry.

*eve* stripe 2 enhancer. We propose a model in which DNA-bound Kr associates with dSAP18 and thereby tethers dHDAC1 at the respective loci to silence target genes by local histone deacetylation.

## EXPERIMENTAL PROCEDURES

**Fly Genetics**—The following fly stocks were used: *b pr cn wx Kr<sup>JF-1</sup>* (Tübingen stock collection), the balancers *y,w; Sco/CyO*, *P(hb-lacZ)* and *y,w; Ly/TM3, Sb*, and *hs-Kr/CyO, P(hb-lacZ); h7-lacZ* (for details see Ref. 24). The *+ /CyO, P(hb-lacZ); h7-lacZ* fly stock was generated from *hs-Kr/CyO, P(hb-lacZ); h7-lacZ* and *y w; Ly/TM3, Sb* flies to obtain the genotype *+ /CyO, P(hb-lacZ); h7-lacZ*. The P element insertion G13322 (*dsap18<sup>w+,EP</sup>*) was obtained from the GenExel fly stock center. *sap18<sup>R7-18</sup>/TM3, ftz-lacZ* and *sap18-14/TM3, ftz-lacZ* and the *dSap18* rescue stock *y w; P(y+ dSap18* on the II-chr.); *sap18<sup>R7-18</sup>* were described earlier (26). Germ line clones (27, 28) homozygous for *sap18-14* were generated as described (26) involving *sap18-14/ovo<sup>D1</sup>* virgins that were mated to *sap18-14/TM3, ftz-lacZ* or *hs-Kr/CyO, P(hb-lacZ); h7-lacZ* males.

**Liquid Chromatography-coupled ESI-MS/MS**—Proteins were excised from SDS-PAGE, digested with trypsin (29), and subjected to analysis by HPLC-coupled ESI-MS/MS. HPLC-ESI-MS/MS was carried out under standard conditions on a hybrid triple quadrupole/linear ion trap mass spectrometer (4000 Qtrap; Applied Biosystems) coupled to an Agilent 1100 nano-chromatography system (30). Peptide fragment spectra were searched in the NCBI database using Mascot as search engine. Mass accuracy was 1.4 Da and 400 milli-mass units, respectively, for samples analyzed on the linear ion trap. The peptides were constrained to be tryptic with a maximum of one missed cleavage site. Carbamidomethylation of cysteines and oxidation of methionine residues were considered as variable modifications. The highest scoring peptide from each protein as well as single hit peptides were manually inspected to eliminate the false positives in the data set.

**PepSpot<sup>TM</sup> Microarray Analysis and in Vitro Translation Assay**—Cellulose-bound peptide arrays (31) were prepared by JPT Peptide Technologies GmbH (Berlin, Germany). One peptide array (PepSpot39) contained 39 spots of 14-mer peptides representing the Krüppel protein (amino acids 301–502; see Fig. 1A) with seven amino acid overlaps. A second peptide array (PepSpot54) contained 54 species of partially overlapping 16-mer peptides representing the full-length Krüppel sequence with an overlap length of four amino acids (supplemental Table S1). To prevent oxidation of SH groups, cysteine residues of the PepSpot54 array were replaced by serines.

**In Vitro Translation**—<sup>[35S]</sup>Methionine-labeled full-length dSAP18 was produced from the pETWZ1 plasmid (32) using the TNT<sup>®</sup> T7 quick coupled transcription/translation system (Promega; L1170) supplemented with Redivue<sup>®</sup> PRO-MIX <sup>35S</sup> label (65 Mbq, 1.75 mCi of methionine; Amersham). Prior to incubation with membranes, the <sup>35S</sup>-labeled dSAP18 (80 μl) was diluted five times in TBS buffer (10 mM of Tris-HCl, pH 8.0, 100 mM NaCl) and filtered through a Durapore<sup>®</sup> membrane (Ultrafree<sup>®</sup>-MC, 0.22 micron; Millipore). Unincorporated <sup>[35S]</sup>methionine and low molecular weight solutes were removed by ultrafiltration using the regenerated cellulose filter

(Microcon YM-10; 10,000 molecular weight cut-off) at 4,000 rpm. The PepSpot membranes were blocked with the blocking buffer (Sigma) to minimize nonspecific binding of dSAP18. Autoradiographs were obtained after exposure for 40 h, followed by scanning with the Typhoon<sup>TM</sup> 8600 laser-scanner (Molecular Dynamics). Signal quantification was done with a QuantityOne<sup>TM</sup> software tool (Bio-Rad).

As a control, dSAP18 was tagged with an N-terminal His<sub>6</sub> epitope and expressed in a coupled TNT *in vitro* system as described above (except that nonradioactive methionine was added) using the pETWZ2 plasmid as a template. The peptide spots bound by the His<sub>6</sub>-dSAP18 were visualized by mouse monoclonal anti-His<sub>6</sub> primary antibodies (DIA900; Dianova) followed by goat anti-mouse HRP-conjugated secondary antibody detection (Pierce). Enhanced luminescence was recorded by CCD-based Lumi-Imager<sup>TM</sup> (Roche Applied Science).

**Heat Shock and TSA Treatments**—Embryos were collected (100 min; 23 °C) from flies bearing a single *Kr* cDNA transgene under control of the heat-inducible hsp70 promoter balanced over a *CyO* balancer chromosome carrying a *hb-lacZ* transgene (second chromosome) and two *h7-lacZ* transgenes (third chromosome). The embryos were aged (20 or 60 min; 23 °C), dechorionated, and permeabilized (20–30 s) with octane (Fluka) (33) and incubated in a 30 μM TSA (Biomol; dissolved in dimethyl sulfoxide) solution of 1× phosphate-buffered saline solution. Control embryos were treated in parallel but without TSA. The embryos were either exposed to 37 °C (30–60 min) or kept at room temperature (23 °C). After recovery (20 min; 23 °C), the embryos were fixed (*in situ* hybridization) or snap-frozen (liquid nitrogen, RNA isolation, Western blot analysis). For heat shock-induced *Kr* expression in maternal dSAP18 mutant embryos, the embryos were collected from a cross of females with homozygous dSAP18 mutant germ lines and males bearing the *hs-Kr* and *h7-lacZ* transgenes.

**Whole Mount in Situ Hybridization and Antibody Staining**—*lacZ* and *eve* expression were examined by *in situ* hybridization to whole mount preparations using antisense RNA probes as described (14). *Kr* expression was monitored by staining embryos with rabbit-raised anti-*Kr* antiserum followed by staining with goat anti-rabbit Cy2-conjugated fluorescent antibody (Dianova).

For chromatin immunoprecipitation, affinity-purified anti-acetyl K<sup>9,14</sup>histone 3 rabbit polyclonal antibodies (Millipore-Upstate) were used. Western blots and PepSpot39 binding assays were performed with anti-His<sub>6</sub> mouse monoclonal antibody (Dianova). Affinity-purified anti-histone H2A serum, anti-acetylK9, and anti-acetylK14 histone 3 rabbit polyclonal antibodies (Millipore-Upstate) were used for quantitative Western blot experiments. Goat anti-mouse HRP-conjugated antibody and goat anti-rabbit HRP-conjugated antibody (Pierce) were employed as secondary antibodies. For *in situ* detection of protein and digoxigenin-labeled RNA probes, we used anti-*Kr* rabbit polyclonal antiserum, goat anti-rabbit Cy2-conjugated antibodies (Dianova), alkaline phosphatase-conjugated anti-digoxigenin antibodies (Roche Applied Science), rabbit anti-digoxigenin antibodies (Roche Applied Science), sheep anti-rabbit IgG antibodies, and donkey anti-sheep IgG biotinylated antibodies.

## Mode of Transcriptional Repression by Krüppel

*In Silico Analysis and Statistical Methods*—*In silico* prediction of nucleosome patterns at the *h* stripe 7 and *eve* stripe 2 elements (including the respective 10-kb flanking regions) were carried out using the available nucleosome/DNA interaction models (34) and the *Genomica* software tool. To test the significance of differences between medians representing relative enrichment factors as revealed by xChIP analysis via semi-quantitative PCR, the Kruskal-Wallis nonparametric statistical test was used (Analyze-it®, standard edition, v.2.03, Analyze-it Software, Ltd.).

*In Vitro Pulldown Experiments*—GST-(N)Kr<sup>2–502</sup> aa. fusion protein was produced as described (14). Constructs expressing different fragments of Kr fused N-terminally to the GST moiety were produced using primer pairs containing either EcoRI (forward primers) or XhoI (reverse primers) sites (supplemental Table S2) for cloning into the pGEX-4T-3 (Amersham Biosciences). Kr sequences were fused N-terminally to GST via the thrombin sensitive linker. The constructs were expressed in *Escherichia coli* BL21 bacterial cells (see Ref. 14) to produce the respective GST-Kr fusions. The proteins were purified by binding to GSH-Sepharose 4B affinity resin (Pharmacia) and washed under moderate stringency conditions (20 mM HEPES, pH 8.0, 300 mM NaCl, 0.1 mM ZnSO<sub>4</sub>, 0.1% Triton X-100, 4% glycerol). The amount of GSH-Sepharose for binding was adjusted to yield resins containing GST-Kr (concentration of 1 mg/ml). Fusion protein was covalently fixed to the affinity resin (homobifunctional imidoester cross-linker, dimethyl adipimidate; Pierce) and processed according to the instructions of the manufacturer.

*Drosophila* S2 Schneider cells were grown to confluency (0.5–1 × 10<sup>8</sup> cells), harvested into a 50-ml Falcon tube, washed twice with phosphate-buffered saline, and cross-linked with 10 mM of dimethyl adipimidate (room temperature). The cells were disrupted in 1× phosphate-buffered saline (containing protease inhibitors (Roche Applied Science), 5% glycerol, and 1 mM of dithiothreitol) by sonication with ultrasound (five bursts; 30 s each). Triton X-100 was added to 0.05%. Cell debris was removed by centrifugation. Lysate was passed through the sterile filter (pore size, 0.2 μm). Prior to incubation with the GST-Kr-bound resins, the lysates were depleted of GST-interacting molecules by three incubations with excess amounts of the GST-bound resin. Resins loaded with GST-Kr fusion protein were incubated with preconditioned lysate (2 h, 4 °C, constant agitation), collected by a short spin, and washed with several changes of buffer (20 mM HEPES, pH 8.0, 300 mM NaCl, 0.2% Triton X-100, 5% glycerol, 1 mM dithiothreitol, protease inhibitor mixture). GST-Kr bound proteins were eluted with a buffer containing 100 mM of glycine, pH 2.5, precipitated with 20% trichloroacetic acid (Sigma), flushed with 100% acetone (–20 °C), air-dried, redissolved in the Laemmli buffer, and separated by SDS-polyacrylamide gel electrophoresis. The proteins were stained with fluorescent dye SYPRO<sup>R</sup> Ruby (Molecular Probes, S-12000), visualized by the Lumi-Imager<sup>TM</sup> (Roche Applied Science), and processed for mass spectrometry.

His<sub>6</sub>-dSAP18 (amino acid region 11–150) fusion protein was produced in the *E. coli* BL21 cells using a pET28a-vector. His-tagged fusion protein was purified by nickel-nitrilotriacetic acid-Sepharose CL-6B matrix (Qiagen). For pull-down assays, 4

μg of imidazol-eluted protein was incubated with 15-μl resin aliquots loaded with 15 μg of either GST or GST-Kr. Incubations were carried out in 0.5 ml of binding buffer (20 mM Tris-HCl, pH 7.5, 0.15 M NaCl, 0.1 mM ZnSO<sub>4</sub>, 1 mM dithiothreitol, 0.1% Triton X-100, and protease inhibitors) containing 3% bovine serum albumin as nonspecific competitor (2 h, 4 °C). After incubation, resins were centrifuged and washed five times with binding buffer. The proteins were eluted (boiling in 20 μl of 2× Laemmli buffer) and separated by 13.5% SDS-PAGE followed by Western blotting (anti-His<sub>6</sub> mouse monoclonal antibodies, DIA900; Dianova), visualized by goat anti-mouse HRP-conjugated secondary antibodies (Pierce). Enhanced luminescence was induced using SuperSignal<sup>®</sup> West Dura Extended Duration Substrate (Pierce). The signals were visualized on Kodak BioMax XAR film.

*Chromatin Immunoprecipitation and Semi-quantitative PCR*—Chromatin was prepared from ~500 μl of 110–230-min-old embryos. Immunoprecipitations of cross-linked chromatin (14) were carried out with affinity-purified anti-acetyl K<sup>9,14</sup>histone 3 rabbit polyclonal antibodies (Millipore-Upstate; about 3000 ng/ml). 100 μl of Affi-Prep<sup>®</sup> protein A support beads (Bio-Rad) were used to adsorb the antibody-chromatin complexes from 10 ml of immunoprecipitation solution, resulting in between 300 and 500 ng of immunoprecipitated DNA/500 μl of embryos.

Primers to amplify *h* stripe 7, *eve* stripe 2 or *dSec23* sequences are listed in supplemental Table S2. To estimate enrichment of full-length sequences of the *eve2* (772 bp) and *h7* (799 bp) enhancers, as well as the quantification of the small genomic fragments (sizes around 200 bp; see Fig. 5, C and D), semi-quantitative PCR was performed as described (14). The relative enrichment (vertical axis values in the Fig. 5, D and G) was calculated as  $(w/x)/(y/z)$ , where *w* is the ChIP target fragment, *x* is the ChIP reference fragment, *y* is the input target fragment, *z* is the input reference, and all values are the sums of pixel intensities for each band (local background was subtracted). The numbers reflect the relative immunoprecipitation efficiency; values less than 1 are not unexpected. The increased acetylation in response to TSA (Fig. 5E, gray bars) was calculated as  $[(w/x)/(y/z)]^{\text{with TSA}}/[(w/x)/(y/z)]^{\text{no TSA}}$ . The relative sensitivity to sonication (Fig. 5E, black bars) was calculated as  $(y/z)^{\text{no TSA}}/(y/z)^{\text{with TSA}}$ . To increase the range of the exponential amplification phase, PCR was paused after 18 cycles of the following conditions: 40 s at 95 °C, 40 s at 54 °C, and 90 s (600–900-bp fragments) or 30 s (200-bp fragments) at 72 °C. The reaction mix was diluted twice with freshly activated 1× PCR Mastermix (total volume, 50 μl) prior to adding 12 cycles (conditions as described above). Each reaction was done in triplicate. PCR fragments were size fractionated on polyacrylamide gels and stained with EtBr followed by imaging and signal quantification (Lumi-Imager<sup>TM</sup>; Roche Applied Science). PCR products were controlled by sequencing.

*Quantitative Western Blots*—Embryos (50-μl aliquots) were thawed in 300 μl of Laemmli buffer, ground, and heated (95 °C, 10 min). Aliquots of the supernatant with equal amount of protein were separated by 15% SDS-PAGE and transferred to a nitrocellulose membrane (Millipore). The membranes were stained (0.1% Ponceau S; Sigma; in 5% acetic acid) to estimate

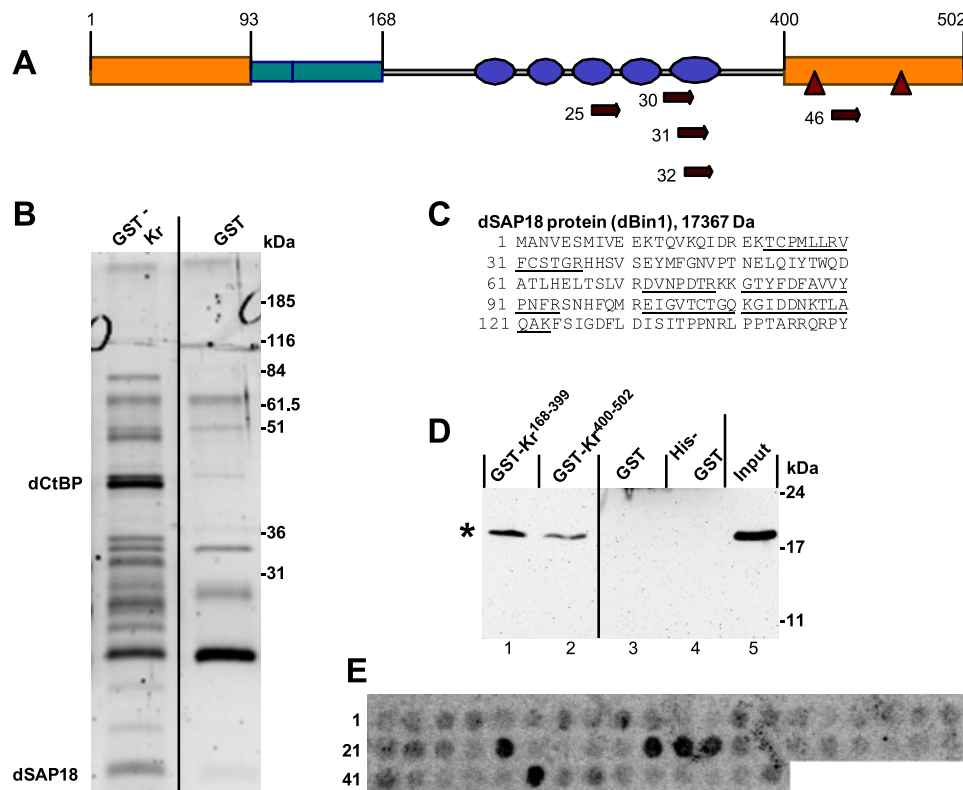


FIGURE 1. **dSAP18 is a Kr binding protein *in vitro*.** **A**, schematic representation of the Kr protein showing the N- and C-terminal transrepressor domains (regions 1–93 and 400–502; orange), the transactivator and coactivator domains (region 93–168; green), the five zinc finger motifs (ovals; blue), the dCtBP-binding sites (positions 414–420 and 464–469; triangles), and the five dSAP18 *in vitro* binding peptides (details in **E**; arrows plus numbers). **B**, SDS-PAGE showing the proteins bound to GST-fused full-length Kr (GST-Kr) and GST control protein, respectively. GST-Kr-specific proteins were submitted to MALDI-TOF-MS analysis, and the previously known Kr-binding protein dCtBP and dSAP18 (see **C**) were identified. Apparent molecular masses (kDa) are indicated. **C**, amino acid sequence of dSAP18 showing Kr-associated peptides as revealed by combined mass spectrometry/Mascot data base analysis. **D**, Western blots of proteins from pull down experiments. Staining with His tag antibodies showing that recombinant His-tagged dSAP18 is bound to Kr. Lane 1, Kr region 168–399. Lane 2, Kr region 400–502. Lane 3, control experiment; dSAP18 does not bind to His-GST. Lane 4, control experiment lacking the His<sub>6</sub>-SAP18 input. Lane 5, His-tagged dSAP18 input. The asterisk indicates the position of His-tagged dSAP18; kDa of marker proteins are indicated. **E**, autoradiograph of peptide spots covering the full-length Kr sequence; spots 1–54 for sequences; supplemental Table S1) after incubation with [<sup>35</sup>S]methionine-labeled dSAP18. Position of dSAP18-binding peptides 25, 30–32, and 46 within Kr is shown in **A**. For details see text.

the protein content and probed with either anti acetylK<sup>9</sup>H3 or anti acetylK<sup>14</sup>H3 antibody (Millipore). ECL was quantified with LAS-1000 (Fujifilm). As controls, the antibodies were removed with Restore™ Western blot stripping buffer (Pierce) and reprobed with anti-histone H2A antibodies (catalog number 07-146; Upstate).

## RESULTS

**Krüppel Binds dSAP18 *in Vitro***—To identify proteins that interact with the transcription factor Kr (Fig. 1A), we isolated proteins from crude extracts of *Drosophila* S2 Schneider cells that bind to a GST-Kr fusion protein. The GST-Kr-associated proteins were identified by liquid chromatography coupled ESI-MS/MS subsequent to SDS-PAGE (Fig. 1B). The Kr-bound proteins included dCtBP (35) and dSAP18 (also called dBin1 (Bicoid-interacting protein 1)), a transcriptional corepressor known to be active during early *Drosophila* embryogenesis (26). Because Kr was shown to require an unknown corepressor in addition to dCtBP (24), we asked whether dSAP18 could serve this function.

Previous results had shown that such a factor must bind to a region N-terminal to the dCtBP-binding domain of Kr (24). To determine the SAP18-binding region of Kr, we used pull-down experiments involving a set of GST fusions that contain various parts of Kr. We confirmed that dCtBP binds to the C-terminal portion (amino acids 400–502) of Kr (22, 23), whereas dSAP18 binds to the amino acid region 168–399, which includes the C<sub>2</sub>H<sub>2</sub> zinc finger domain (Fig. 1A). MALDI-TOF-MS control experiments identified N-terminal peptides of dSAP18 that were associated with full-length Kr (Fig. 1C) but not with GST fusions that lack the Kr<sup>168–399</sup>-region, and pull-down experiments with bacterially expressed His-tagged dSAP18 protein confirmed strong *in vitro* binding of dSAP18 to the central region of Kr (amino acid region 168–399) as well as weak binding to the C-terminal part (Fig. 1D). We also expressed GST fusions containing the N-terminal region of Kr, but they were not soluble under the conditions used for the other GST fusions of Kr. Thus, we cannot exclude the possibility that dSAP18 is capable of binding also to the N-terminal portion of Kr.

To determine the dSAP18-binding sites of Kr, we performed peptide array analysis employing tiled 16-mer peptides (see supplemental material), which cover the entire Kr sequence (peptides 1–54; Fig. 1E). *In vitro* translated [<sup>35</sup>S]methionine-labeled dSAP18 bound strongly to three overlapping peptides (peptides 30–32; Fig. 1E) that contain the region <sup>342</sup>KFRRR<sup>346</sup> of the fifth zinc finger motif of Kr. Two additional sites were found in the third zinc finger motif (<sup>293</sup>LRRHLRVH<sup>300</sup>, peptide 25) and the C-terminal domain (amino acid interval <sup>431</sup>NIARRKAQ<sup>438</sup>, peptide 46), respectively (Fig. 1, A and E). A complementary immunological approach with His-tagged dSAP18 confirmed the identified binding sites (data not shown). To exclude the possibility that dSAP18 binds to a short stretch of basic amino acids in an unspecific manner only, we also tested a total of 14 arbitrary peptides of comparable basicity. No binding was observed except when the consensus sequence RR(K/R)H(H/K) was present in target peptides. This motif was found in a number of *Drosophila* transcription factors including Bicoid, which was previously shown to functionally interact with dSAP18 (26). A detailed analysis of the dSAP18-binding sites in *Drosophila* transcription factors and their functional requirement will be presented else-

## Mode of Transcriptional Repression by Krüppel

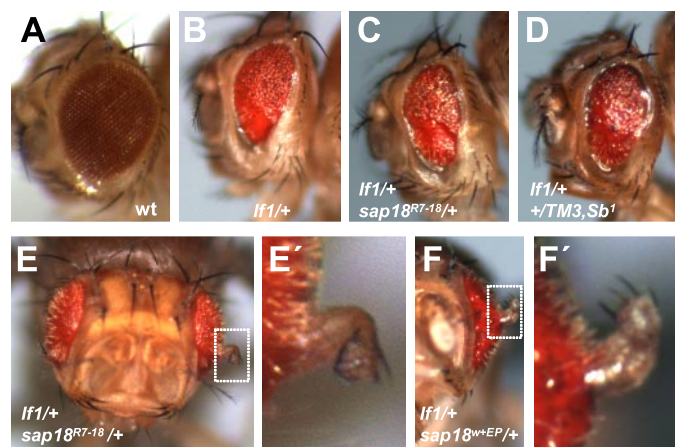


**FIGURE 2. Loss of maternal *dSap18* activity generates transformations of eye structures in the dominant *Kr* mutant (*If*) and suggests an epigenetic maternal effect of *dSAP18* on *Kr* function.** *A*, light micrograph of an adult wild type eye. *B*, dominant *Kr* mutant (*If-1/+*) eye. Note that *If* causes a slit-like rough eye phenotype. *C–F*, flies from matings of *If-1/If-1* males and either *sap18<sup>R7-18</sup>/TM3,Sb<sup>1</sup>* (*C–E*) or *sap18<sup>w+EP</sup>/TM3,Sb<sup>1</sup>* (*F*) females. *C* and *D*, eyes of *If-1/+; sap18<sup>R7-18</sup>/+* (*C*) and *If-1/+; +/TM3,Sb<sup>1</sup>* (*D*) individuals showing that *sap18<sup>R7-18</sup>* or balancer chromosomes used in the crossings do not alter the *If* phenotype. *E* and *F*, transformations of eye structures observed in about 2% of *If-1/+; sap18<sup>R7-18</sup>/+* (*E*) and *If-1/+; sap18<sup>w+EP</sup>/+* (*F*) individuals (not seen in more than 500 *If-1/+; +/+* or *+/+; sap18/+* mutant flies. *E'* and *F'*: enlargements of areas marked by dotted lines in *E* and *F*.

where.<sup>3</sup> We also note that the binding of *Kr* sequences and *dSAP18* withstands salt concentrations up to at least 300 mmol (see “Experimental Procedures”). Taken together, our results indicate that *dSAP18* can bind *Kr* *in vitro* and that the binding involves distinct binding sites.

**Genetic Interactions Suggest That *SAP18* and *Kr* Interact *in Vivo***—To establish a functional basis for an interaction between *Kr* and *dSap18*, we performed genetic studies using a loss-of-function mutant allele, *sap18<sup>R7-18</sup>* (26) and the dominant *Kr* gain-of-function mutation *If* (Irregular facets) (13). *If* causes ectopic *Kr* activity in the developing eye imaginal discs, resulting in a dosage-dependent slit-like eye phenotype (13). The *If* mutant phenotype is modified in response to reduced activity of zygotically expressed genes that act in the same developmental pathway (12, 13), and it responds to reduced maternally expressed gene activities, resulting in an outgrowth of transformed adult eye tissue (36). Such transformations are observed in low frequency, providing evidence for an epigenetic “inherited maternal effect” caused by histone acetylation/deacetylation events (36). *sap18<sup>R7-18</sup>* mutants alone have no scorable effects on eyes.

Crosses between the *If-1* homozygous males and heterozygous *sap18<sup>R7-18</sup>* or *sap18<sup>w+EP</sup>* females did not alter the *If* mutant phenotype (Fig. 2, *A–D*) but resulted in transformations in about 2% of the offspring (Fig. 2, *E* and *F*). No transformation was observed in more than 500 individuals resulting from reciprocal crosses between heterozygous *sap18* males and *If-1* females. Thus, the modifier effect was neither allele-specific nor dependent on the genetic background of the female flies, and it was not due to reduced zygotic *dSap18* activity. It can be attributed to an earlier reported maternal effect, likely to

involve epigenetic events such as histone acetylation/deacetylation events (36). These results highlight that *SAP18* not only interacts with *Kr* *in vitro* but could also play a role in one or several *Kr*-dependent gene regulation processes *in vivo*.

***dSAP18* and *Kr*-dependent Regulation of *h* Stripe 7 but Not *eve* Stripe 2**—During the blastoderm stage, *Kr* binds to and represses via the *eve* stripe 2 element (18, 37) in a *dCtBP*-dependent manner (22). It also binds to the *h* stripe 7 element and represses *h* stripe 7 expression in a *dCtBP*-independent manner (24), indicating that *Kr*-dependent repression involves more than one mechanism (24).

Previous studies of Singh *et al.* (26) suggested that the absence of *dSAP18* activity did not interfere with the spatial pattern of embryonic *eve* or *h* expression. However, this finding does not rule out the possibility that *dSAP18* participates in *Kr*-dependent repression. It could be that *dCtBP* and/or the activity of other corepressors are sufficient to mediate *Kr*-dependent repression in the absence of *dSAP18* and that the corepressors may act, at least in part, redundantly. To test this possibility and to explore whether *dSAP18* functions as a corepressor on *Kr* target genes, we examined *eve* expression in wild type and *dSAP18*-deficient embryos after heat shock-induced *Kr* expression during blastoderm formation. In wild type embryos (Fig. 3, *A–C*), ubiquitous *Kr* overexpression caused full repression of *eve* stripes 1–5, whereas in some embryos weak *eve* stripe 6 and 7 expression remained (Fig. 3*C'*). Thus, anterior *eve* stripes are more sensitive to *Kr*-dependent repression than posterior stripes. In the absence of maternal *dSAP18* activity, no effect could be observed on *Kr*-dependent *eve* stripe 2 and 5 repression, but *eve* stripes 1, 3, and 4 were derepressed (Fig. 3, *D–F* and *F'*). The *lacZ* reporter transgenes (as described below and in Fig. 3 legend) used to identify embryos of particular genotypes had no effect on the *eve* expression. These results show that *dSAP18* is not required for *Kr*-dependent repression of *eve* stripes 2 and 5 but to various degrees for the repression of the other *eve* stripes.

We next asked whether *dSAP18* contributes to *Kr*-dependent hairy stripe 7 repression, which does not require *dCtBP* (24). We used a transgene that consists of a *lacZ* reporter under the control of the *h* stripe 7 minimal enhancer (24) and mediates either full repression in response to overexpressed full-length *Kr* or partial repression in response to truncated *Kr* (region 1–351 in *Kr<sup>v</sup>* mutant), which lacks the two *dCtBP*-binding sites (24) as well as one of the three *in vitro* identified *dSAP18* sites. In the absence of maternal *dSAP18*, overexpression of *Kr* in response to 30 min of heat shock induction was unable to repress the *h7-lacZ* reporter gene (Fig. 4, *A–F*). However, prolonged expression of *Kr* (60 min) caused repression of the *h7-lacZ* reporter in *dSAP18* mutant embryos (Fig. 3, *F* and *F'*). These observations indicate that *dSAP18* can indeed participate in the *Kr*-dependent repression of the *h7-lacZ* gene. In the presence of high levels of *Kr*, as obtained after its prolonged expression for 60 min, however, *Kr*-dependent repression can also occur by a mechanism that does not involve *dSAP18*. In contrast, the *eve* stripes 1, 3, and 4 remain unsuppressed in response to the prolonged expression of *Kr* as shown in Fig. 3 (*C* and *C'*).

<sup>3</sup> A. Matyash and H. Jäckle, manuscript in preparation.

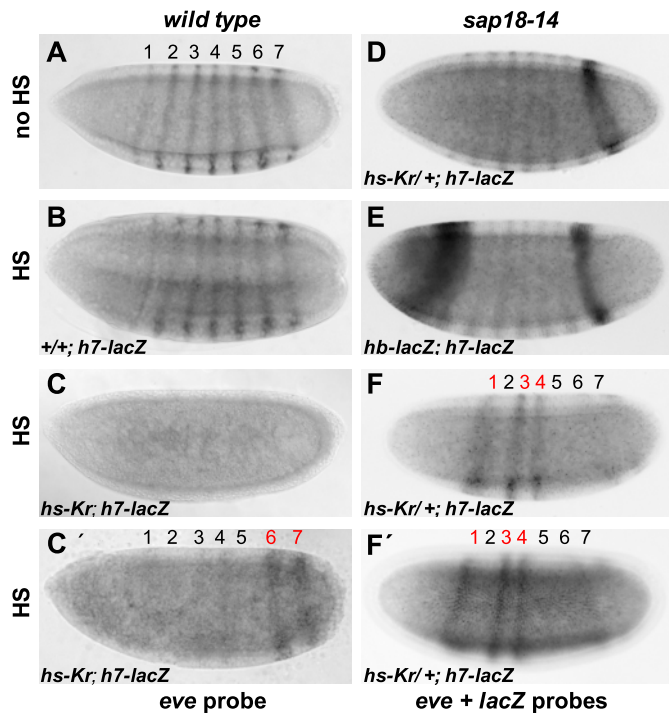


**FIGURE 3. *eve* and *h7* expression in wild type and dSAP18-lacking embryos in response to heat shock induced ectopic Kr activity (60 min; 37 °C).** A–C, whole mount preparations of *hb-lacZ* (or *hs-Kr*) and *h7-lacZ* containing wild type blastoderm embryos. D–F, embryos lacking maternal dSAP18 activity (obtained through dSAP18 mutant female germ line clones; see “Experimental Procedures”). Embryos (anterior to the left, dorsal side up) were *in situ* hybridized with an *eve* probe (A–C and C') or with combined *eve* and *lacZ* probes. Note the seven stripe expression pattern of *eve* in wild type (A) and dSAP18-deficient (D) embryos. No change of expression occurs in response to heat shock (HS) (B), when maternal dSAP18 is absent (D) or in response to heat shock when both maternal dSAP18 and the *hs-Kr* transgene are absent (E). Note that *h7-lacZ* expression is not affected by the absence of dSAP18 (D) and by heat shock treatment alone (E). *eve* expression is strongly repressed or abolished (majority of embryos) in response to heat shock-induced Kr expression (C). The two posterior stripes (stripes 6 and 7; red) are more resistant to Kr activity than the anterior stripes. F, in embryos lacking maternal dSAP18, *eve* stripes 2 and 5–7 are repressed by heat shock-induced Kr, whereas *eve* stripes 1, 3, and 4 expression are not. *h7-lacZ* expression is strongly reduced after the 60-min heat shock-induced Kr expression (compare E and F). For details see text and Fig. 4 for Kr-dependent *h7-lacZ* repression after 30 min of heat shock.

**SAP18-dependent Repression by Kr Involves Histone Deacetylation**—SAP18 interacts with SIN3A, a component of the dSin3A/dRpd3 dHDAC1 (25). RNA interference experiments with *Drosophila* cell culture and transcriptional profiling indicates that the transcriptional effects of the HDAC-inhibitor TSA are due to inhibited dHDAC1 activity that results in increased acetylation of histone 3 (H3) on lysine 9 and 14 (38, 39). To test the possible link between Kr-dependent repression and SAP18-mediated H3 deacetylation, we examined the effect of TSA on Kr-overexpressing embryos. In the presence of TSA, Kr-overexpressing embryos did not repress expression of *h7-lacZ* (Fig. 4H and supplemental Fig. S2), suggesting that *h* stripe 7 repression by Kr involves H3 deacetylation. This idea was further studied using acetylK<sup>9</sup>H3- and acetylK<sup>14</sup>H3-specific antibodies. TSA treatment caused a strong increase of K<sup>9,14</sup>H3 acetylation in wild type embryos, whereas in Kr-overexpressing embryos, this effect was strongly reduced (supplemental Fig. S1). In addition, in the absence of TSA, the level of

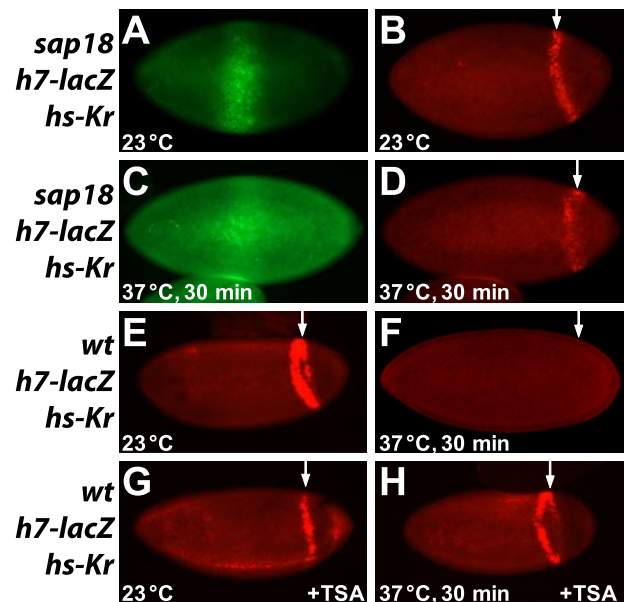


**FIGURE 4. Kr-dependent *h7-lacZ* repression in embryos lacking maternal dSAP18 and dHDAC1 activities and their response to heat shock-induced Kr (30 min, 37 °C).** Blastoderm embryos (anterior to the left; dorsal up) were double stained with anti-Kr antibodies (green) and *lacZ* antisense RNA (red) (A–D) or with *lacZ* antisense RNA only (E–H). A–D, the embryos lacking maternal dSAP18 activity. E and F, control embryos containing the *hs-Kr* transgene. The arrows indicate the positions of the posterior *h7-lacZ* expression domain. Kr (A and C) and *h7-lacZ* expression (B and D) in the embryos lacking maternal dSAP18 with (D) or without (B) heat shock-induced Kr activity. Note reduced *h7-lacZ* repression in D; a corresponding wild type (wt) embryo is shown in F. E and F, wild type embryos bearing *h7-lacZ* and *hs-Kr* transgenes at room temperature (E) or after heat shock-induced Kr, which abolishes *h7-lacZ* expression (F). G and H, wild type embryos treated with TSA (30 μM) without (G) or in the presence of heat shock-induced Kr (H; see also supplemental Fig. S2). Note that Kr does not repress *h7-lacZ* expression when HDAC1 activity was blocked (compare F and H).

acetylK<sup>9</sup>H3 in embryos overexpressing Kr was lower than in wild type embryos (supplemental Fig. S1).

**Kr-dependent Deacetylation at the *h* Stripe 7 but Not the *eve* Stripe 2 Element**—We next asked whether a lack of Kr-dependent repression of *h7-lacZ* correlates with an increased K<sup>9,14</sup>H3 acetylation at the *h* stripe 7 element. We performed immunoprecipitation experiments with anti-acetylK<sup>9,14</sup>H3 antibodies and chemically cross-linked chromatin from Kr-overexpressing *Drosophila* embryos that contain a *h7-lacZ* transgene either in the presence or the absence of TSA. Immunoprecipitated chromatin was examined by PCR for enrichment of *eve* stripe 2 element sequences, which are regulated by Kr in a dCtBP-dependent manner, and *h* stripe 7 element sequences, which are regulated by Kr in a dCtBP-independent manner. Relevant DNA-binding sites of the *eve* stripe 2 and *h* stripe 7 elements, as well as the nucleosome distribution as revealed by the *Genomica* software (see Ref. 34), are shown in Fig. 5 (A and B). For control chromatin that lacks Kr DNA-binding sites, we used exon 2 of *dSec23*.

Prior to DNA extraction and PCR amplification, embryos were sonicated to break cells and nuclei and shear chromatin. In the absence of TSA and in response to 30 min heat shock-induced Kr expression, we found that the *h7* element sequences were significantly enriched over *eve* stripe 2 and the control sequences (Fig. 5C; for a 23 °C control see Fig. 5F). We attribute

# Mode of Transcriptional Repression by Krüppel

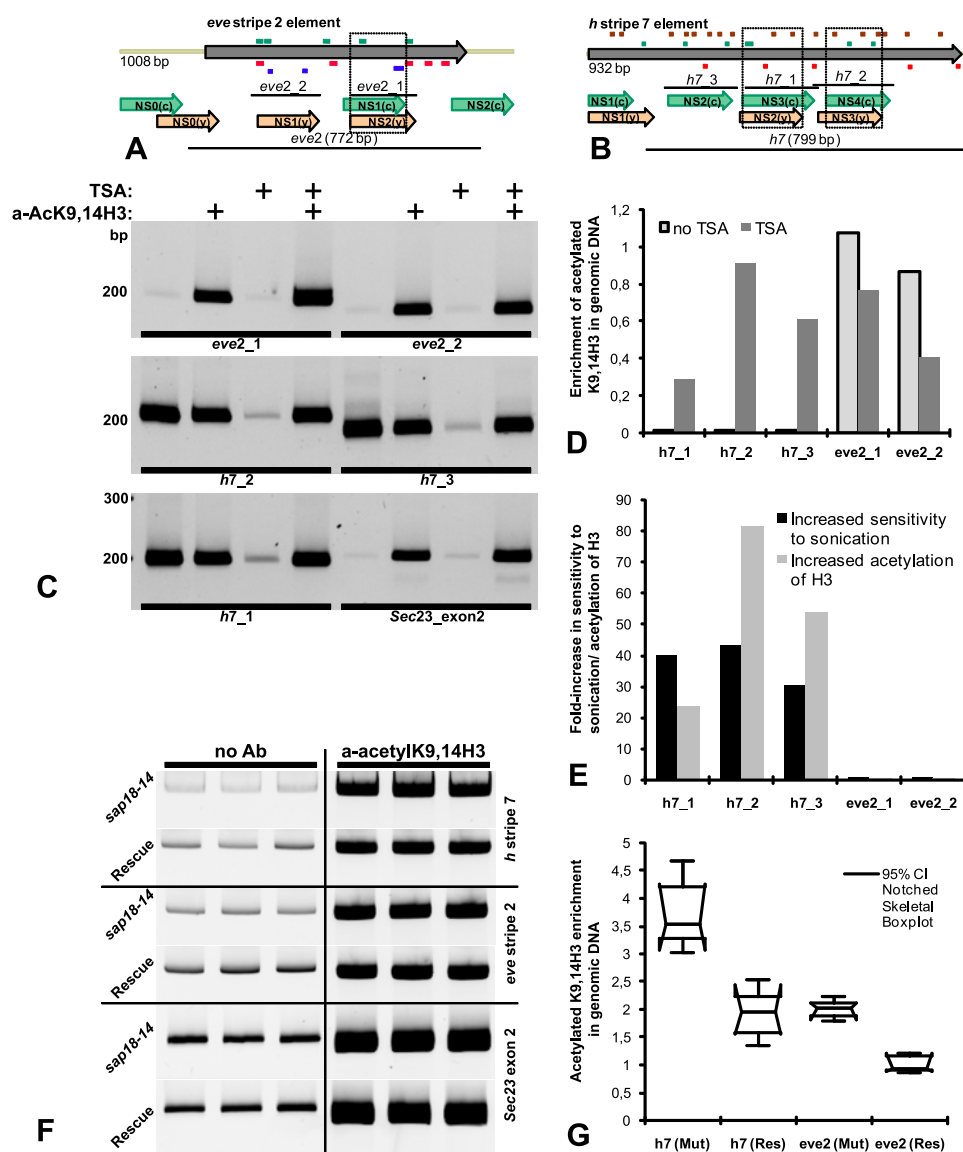


**FIGURE 5. Acetylation of histone H3 at *h7* and *eve stripe 2* enhancer elements in response to *Kr* activity, inhibition of dHDAC1, and reduced maternal dSAP18 activity.** *A* and *B*, schematic representation of the *eve stripe 2* (*A*) and *h stripe 7* (*B*) enhancers. Binding sites for *Kr* (red; (18, 24)), *Giant* (blue; (17, 18, 37)), *Bicoid* (green; (18, 21)) and *Caudal* (brown; (21)) are shown. Primers used to amplify enhancer regions (*C* and *F*) are listed in supplemental Table S2. Predicted positions of stable nucleosomes (*NS*; stability probability > 0,2; (34) are marked (green, chicken model, NS0–4,c; brown, yeast model, NS0–3,y); regions designated according to both models are framed (dotted lines). Note that the *h stripe 7* element contains a denser array of nucleosomes than the *eve stripe 2* element (for details see text and “Experimental Procedures”). *Black bars*, amplified regions of the *eve stripe 2* and *h7* enhancers in *C–E*. *C–E*, xChIP analysis showing  $K^9/K^{14}$  acetylation of histone H3 in the *eve stripe 2* and *h7* enhancers (*black lines* in *A* and *B*) in response to overexpressed *Kr* and the HDAC1-inhibitor TSA (30  $\mu$ M), respectively. *C*, chromatin isolated after immunoprecipitation with anti-acetyl $K^9/K^{14}$ H3 antibodies (+) from TSA treated (+) or untreated (–) embryos. DNA of the *eve stripe 2* and *h7* enhancers were amplified by PCR; control PCRs were carried out with *dSec23* DNA, which lacks *Kr*-binding sites. *D–E*, quantification of the xChIP results shown in *C* (see “Experimental Procedures” for details). Note that  $K^9/K^{14}$  acetylation of histone H3 is increased at the *h7* after TSA treatment and heat shock-induced *Kr* activity but not at the *eve stripe 2* enhancer (*D* and *E*). The effect correlates with increased sensitivity to ultrasound treatment (*E*; *black bars*).  $K^9/K^{14}$  acetylation at the three subregions of the *h7* element is strongly reduced in response to *Kr*, and this effect is reverted by TSA treatment. *F* and *G*, ChIP analysis (*F*) and quantification of the  $K^9/K^{14}$ H3 acetylation (*G*) at the *eve2* and *h7* enhancers from heterozygous *dSAP18* females (*sap18-14, Mut*) or from females that contain two copies of the *dSAP18* transgene (*Rescue, Res*) at the 772-bp *eve stripe 2* enhancer (*black line* in *A*), the 799-bp *h stripe 7* enhancer (*black line* in *B*), and the *Sec23* control sequences, respectively. Note that  $K^9/K^{14}$  acetylation at the *h stripe 7* enhancer is about twice as high as at the *eve stripe 2* element ( $p < 0,0001$ ) and that H3 deacetylation in response to two *dSAP18* transgenes (*Res*) is enhanced accordingly. The 95% notched skeletal box plot shows the calculated median value (horizontal line within the box) for the relative enrichments and the corresponding 95% CI of the median (notched part); the error bars show the limits of the data spread. A nonparametric Kruskal-Wallis test was used to assess the significance of the differences in the group of four medians, all pair-wise (Bonferroni protected). The details are outlined under “Experimental Procedures.”

this effect to a lower sensitivity of *h7* element sequences to sonication as compared with *eve stripe 2* and the control sequences. These findings suggest that *h7* element sequences are better protected against sonication than *eve stripe 2* sequences, perhaps as a result of chromatin compaction that might occur on the *h7* element as a result of *Kr*-dependent deacetylation in response to HDAC activity (40). Indeed, ChIP experiments (Fig. 5, *C–E*) showed that TSA treatment of *Kr*-overexpressing embryos caused an increase of  $K^9/K^{14}$ H3 acetylation at the *h7* element. In contrast, TSA treatment of *Kr*-overexpressing embryos did not increase the  $K^9/K^{14}$ H3 acetylation at the *eve stripe 2* element as compared with the *Sec23* control gene. Furthermore, TSA did not lead to any change in sensitivity to sonication. Additional xChIP experiments performed with primer sets directing amplification of the full-length *h7*- and *eve2* elements (data not shown) confirmed the above mentioned results. Collectively, these findings suggest that *Kr*-dependent repression via the *h stripe 7* involves deacetylation of H3, whereas repression via the *eve stripe 2* element does not.

*Maternal dSAP18 Participates in H3 Acetylation at Kr-regulated Enhancers—No effect on *h* and *eve stripe* expression patterns is seen in blastoderm stage embryos lacking maternal dSAP18 activity (26). Thus, dCtBP and other possible corepressors may support repression by *Kr* in the absence of dSAP18. However, *h7-lacZ* expression was only weakly repressed when *Kr* was overexpressed in embryos lacking the maternal complement of SAP18 (Fig. 4D). We therefore asked whether the loss of maternal SAP18 activity in embryos affects  $K^9/K^{14}$ H3 acetylation at the *h stripe 7*, but not at the *eve stripe 2* enhancer sequences. Fig. 5 (*F* and *G*) shows the results of ChIP assays with anti-acetyl  $K^9/K^{14}$ H3 antibodies, indicating that  $K^9/K^{14}$ H3 acetylation in embryo collections obtained from crosses of *sap18-14* heterozygous*

parents was higher at the *h* stripe 7 enhancer as compared with the SAP18-insensitive *eve* stripe 2 enhancer or the *sec23* control gene. This result is consistent with the *in silico* prediction of nucleosome packing (Fig. 5, A and B), suggesting a more dense array of nucleosomes at the *h* stripe 7 enhancer as compared with the *eve* stripe 2 enhancer. In conclusion, both biochemical and functional data suggest that Kr recruits dSAP18-mediated dHDAC1 activity in an enhancer-specific manner.

## DISCUSSION

We provide evidence that Kr exerts transcriptional repression not only by association with the corepressor dCtBP but also by site-specific deacetylation of histones, a mechanism that involves an interaction between Kr and dSAP18. The dual mode of Kr-dependent repression might explain earlier studies showing that Kr represses *eve* stripe 2 expression, but not *h* stripe 7 expression, in a dCtBP-dependent manner (24). Consistent with these observations, a mutant Kr protein that lacks dCtBP-binding sites still associates with dSAP18, which in turn interacts with the Sin3A-HDAC1 repressor complex (26, 41). dSAP18 was also shown to bind the homeodomain transcription factor Bicoid, causing repression of anterior gap genes such as *hunchback* in the late *Drosophila* blastoderm embryo. SAP18-dependent repression involves histone deacetylase both in flies (26, 42) and mammals (41), and SAP18 that links the HDAC1 complex with sequence-specific transcriptional repressors bound to chromatin is also found in plants (43). The results shown here are consistent with such a SAP18-dependent mode of Kr-dependent repression that provides target gene-specific repression. Because both dCtBP and SAP18 are uniformly distributed in the embryo, it will be important to learn how the *eve* stripe 2 and the *h* stripe 7 enhancer distinguish between the dCtBP- or SAP18-dependent modes of repression. One possibility is that differential packing of the enhancer DNA into nucleosomes might account for the difference in susceptibility to the SAP18/HDAC1-mediated repression.

dSAP18 binds to three distinct regions of Kr (Fig. 1A), including the 42-amino acid-long repressor region (21), which is conserved in Kr homologs of all *Drosophila* species. However, as observed for dCtBP, dSAP18 alone cannot account for Kr-dependent repression of *h7-lacZ*, because prolonged expression of Kr is able to overcome the lack of dSAP18 activity as observed for the *h7* element in dSAP18 mutants. Therefore, it is likely that the full spectrum of Kr-dependent repression is mediated redundantly, employing at least two different corepressors that involve different modes of repression.

*In vitro*, dSAP18 binds to the sequence motif<sup>344</sup>RRRHHL<sup>349</sup> of Kr and to a similar motif<sup>(143)</sup>RRRRHKI<sup>(149)</sup> of Bicoid (this study, data not shown); the latter is consistent with the results reported by Zhu *et al.* (42). In both proteins, the dSAP18-binding sites are localized in the C-terminal portion of their DNA-binding domains. Thus, when acting from weak binding sites *in vivo*, transcription factors might be able to form strong complexes with dSAP18. In fact, Bicoid-dependent repression of *hunchback*, which depends on both SAP18 and HDAC1 (26), occurs only at the very anterior tip of blastoderm embryos where the Bicoid concentration is highest and the target gene enhancers contain multiple weak Bicoid-binding sites.

dSAP18 also interacts with the histone-specific H3K27 methyl-transferase E(z) (Enhancer of zeste) (44), a component of the polycomb group protein complex (45, 46), and with the GAGA factor (47), a transcription factor of the trxB (trithorax group) protein complex (48). Thus, dSAP18 is capable of interacting with two regulatory protein complexes that have antagonistic functions in gene regulation. Whereas the polycomb group complex acts as a repressor of homeotic genes in ectopic locations (see reviews in Refs. 49–51), the trxB complex is required for activation and maintenance of their transcription (52). However, this clear-cut distinction between polycomb group and trxB functions has been questioned, because polycomb group and trxB group members were shown to act both as context-dependent repressors and activators of transcription (53), and factors with such dual functions include both the E(z) and GAGA factor proteins (54, 55). In fact, interactions between dSAP18 and GAGA factor at the *iab-6* element of the bithorax complex, for example, were shown to cause transcriptional activation and not repression (47, 56).

Our study suggests that Kr mediates repression through at least two pathways involving either dCtBP or SAP18. dCtBP-dependent and -independent repression of the transcription factors Knirps and Hairless exert quantitative effects (57, 58), whereas Kr distinguishes dCtBP and dSAP18 recruitment at different enhancers. We observed, however, that the loss of SAP18 activity does not affect the pattern of *eve* stripe expression and that prolonged Kr can suppress *h7-lacZ* expression in the absence of dSAP18. Thus, although both dSAP18 and dCtBP act independently from each other, the two corepressors, or other yet unknown corepressors, can functionally substitute for each other under forced conditions. However, their mode of repression appears to involve different mechanisms. One mechanism is exemplified by the dCtBP-dependent repression of *eve*-stripe 2 (22, 23) and not yet established at the molecular level. dCtBP-dependent repression does not act via unleashing local heterochromatinization (59), does not require dHDAC1 activity (60), and is insensitive to the HDAC inhibitor TSA (61). Consistently, coimmunoprecipitation studies failed to detect HDAC activity in the dCtBP immunoprecipitates (62), histone H3 remained acetylated in dCtBP-deficient embryos, and transcription was not repressed (63, 64). Other studies, however, implied an association of dCtBP with HDACs (65, 66). Thus, the mechanism of the dCtBP mode of repression is not yet fully understood.

Our results showing a lack of H3 deacetylation at the *eve* stripe 2 enhancer in response to Kr repression are consistent with the argument that *eve* stripe 2-mediated repression involves the corepressor CtBP. The second, dCtBP-independent mode of Kr-dependent repression, as exemplified by the *h* stripe 7 element (and possibly also *eve* stripes 1, 3, and 4) does require both dSAP18 and HDAC1 activities. In support of this mode of repression, we observed in Kr-overexpressing embryos (i) a dSAP18-dependent loss of K<sup>9,14</sup>H3 acetylation on the *h* stripe 7 element, (ii) an increased resistance of the *h7* enhancer DNA to sonication, and (iii) SAP18-dependent repression of the *h7* reporter gene in response to Kr activity. These Kr-dependent effects were dependent on HDAC1 enzymatic activity as revealed by experiments using the HDAC1 inhibitor, TSA.

## Mode of Transcriptional Repression by Krüppel

Our results therefore suggest that dSAP18-dependent repression by Kr involves structural changes of chromatin, such as compaction or condensation, likely to be caused by site-specific heterochromatization in response to enhancer-specific HDAC1 activity.

*Acknowledgments*—We thank our colleagues in the labs for critical discussions.

### REFERENCES

- Gaul, U., and Jäckle, H. (1990) *Adv. Genet.* **27**, 239–275
- Jäckle, H., Hoch, M., Pankratz, M. J., Gerwin, N., Sauer, F., and Brönnner, G. (1992) *J. Cell Sci. Suppl.* **16**, 39–51
- Rosenberg, U. B., Preiss, A., Seifert, E., Jäckle, H., and Knipple, D. C. (1985) *Nature* **313**, 703–706
- Pankratz, M. J., and Jäckle, H. (1990) *Trends Genet.* **6**, 287–292
- Pankratz, M. J., Seifert, E., Gerwin, N., Billi, B., Nauber, U., and Jäckle, H. (1990) *Cell* **61**, 309–317
- Pankratz, M. J., Hoch, M., Seifert, E., and Jäckle, H. (1989) *Nature* **341**, 337–340
- Stanojevic, D., Hoey, T., and Levine, M. (1989) *Nature* **341**, 331–335
- Hartmann, C., Landgraf, M., Bate, M., and Jäckle, H. (1997) *EMBO J.* **16**, 5299–5309
- Hoch, M., and Jäckle, H. (1998) *EMBO J.* **17**, 5766–5775
- Hoch, M., Schröder, C., Seifert, E., and Jäckle, H. (1990) *EMBO J.* **9**, 2587–2595
- Hoch, M., Seifert, E., and Jäckle, H. (1991) *EMBO J.* **10**, 2267–2278
- Abrell, S., Carrera, P., and Jäckle, H. (2000) *Chromosoma* **109**, 334–342
- Carrera, P., Abrell, S., Kerber, B., Walldorf, U., Preiss, A., Hoch, M., and Jäckle, H. (1998) *Proc. Natl. Acad. Sci. U. S. A.* **95**, 10779–10784
- Matyash, A., Chung, H. R., and Jäckle, H. (2004) *J. Biol. Chem.* **279**, 30689–30696
- Sauer, F., and Jäckle, H. (1991) *Nature* **353**, 563–566
- Sauer, F., and Jäckle, H. (1993) *Nature* **364**, 454–457
- Small, S., Kraut, R., Hoey, T., Warrior, R., and Levine, M. (1991) *Genes Dev.* **5**, 827–839
- Stanojevic, D., Small, S., and Levine, M. (1991) *Science* **254**, 1385–1387
- Berman, B. P., Nibu, Y., Pfeiffer, B. D., Tomancak, P., Celniker, S. E., Levine, M., Rubin, G. M., and Eisen, M. B. (2002) *Proc. Natl. Acad. Sci. U. S. A.* **99**, 757–762
- Sauer, F., Fondell, J. D., Ohkuma, Y., Roeder, R. G., and Jäckle, H. (1995) *Nature* **375**, 162–164
- La Rosee, A., Häder, T., Taubert, H., Rivera-Pomar, R., and Jäckle, H. (1997) *EMBO J.* **16**, 4403–4411
- Nibu, Y., Senger, K., and Levine, M. (2003) *Mol. Cell Biol.* **23**, 3990–3999
- Nibu, Y., Zhang, H., Bajor, E., Barolo, S., Small, S., and Levine, M. (1998) *EMBO J.* **17**, 7009–7020
- La Rosee-Borggreve, A., Häder, T., Wainwright, D., Sauer, F., and Jäckle, H. (1999) *Mech. Dev.* **89**, 133–140
- Zhang, Y., Iratni, R., Erdjument-Bromage, H., Tempst, P., and Reinberg, D. (1997) *Cell* **89**, 357–364
- Singh, N., Zhu, W., and Hanes, S. D. (2005) *Dev. Biol.* **278**, 242–254
- Chou, T. B., and Perrimon, N. (1992) *Genetics* **131**, 643–653
- Chou, T. B., and Perrimon, N. (1996) *Genetics* **144**, 1673–1679
- Shevchenko, A., Wilm, M., Vorm, O., and Mann, M. (1996) *Anal. Chem.* **68**, 850–858
- Deckert, J., Hartmuth, K., Boehringer, D., Behzadnia, N., Will, C. L., Kastner, B., Stark, H., Urlaub, H., and Lührmann, R. (2006) *Mol. Cell Biol.* **26**, 5528–5543
- Frank, R. (2002) *J. Immunol. Methods* **267**, 13–26
- Zhu, W., and Hanes, S. D. (2000) *Gene (Amst.)* **245**, 329–339
- Strecker, T. R., McGhee, S., Shih, S., and Ham, D. (1994) *Biotech. Histochem.* **69**, 25–30
- Segal, E., Fondufe-Mittendorf, Y., Chen, L., Thastrom, A., Field, Y., Moore, I. K., Wang, J. P., and Widom, J. (2006) *Nature* **442**, 772–778
- Nibu, Y., Zhang, H., and Levine, M. (1998) *Science* **280**, 101–104
- Sollars, V., Lu, X., Xiao, L., Wang, X., Garfinkel, M. D., and Ruden, D. M. (2003) *Nat. Genet.* **33**, 70–74
- Small, S., Blair, A., and Levine, M. (1992) *EMBO J.* **11**, 4047–4057
- Foglietti, C., Filocamo, G., Cundari, E., De Rinaldis, E., Lahm, A., Cortese, R., and Steinkuhler, C. (2006) *J. Biol. Chem.* **281**, 17968–17976
- Huang, X., and Kadonaga, J. T. (2001) *J. Biol. Chem.* **276**, 12497–12500
- Mottus, R., Sobel, R. E., and Grigliatti, T. A. (2000) *Genetics* **154**, 657–668
- Cheng, S. Y., and Bishop, J. M. (2002) *Proc. Natl. Acad. Sci. U. S. A.* **99**, 5442–5447
- Zhu, W., Foehr, M., Jaynes, J. B., and Hanes, S. D. (2001) *Dev. Genes Evol.* **211**, 109–117
- Song, C. P., and Galbraith, D. W. (2006) *Plant Mol. Biol.* **60**, 241–257
- Wang, L., Ding, L., Jones, C. A., and Jones, R. S. (2002) *Gene (Amst.)* **285**, 119–125
- Ng, J., Hart, C. M., Morgan, K., and Simon, J. A. (2000) *Mol. Cell Biol.* **20**, 3069–3078
- Tie, F., Furuyama, T., Prasad-Sinha, J., Jane, E., and Harte, P. J. (2001) *Development* **128**, 275–286
- Espinosa, M. L., Canudas, S., Fanti, L., Pimpinelli, S., Casanova, J., and Azorin, F. (2000) *EMBO Rep.* **1**, 253–259
- Farkas, G., Gausz, J., Galloni, M., Reuter, G., Gyurkovics, H., and Karch, F. (1994) *Nature* **371**, 806–808
- Schuettengruber, B., Chourrout, D., Vervoort, M., Leblanc, B., and Cavalli, G. (2007) *Cell* **128**, 735–745
- Schwartz, Y. B., and Pirrotta, V. (2007) *Nat. Rev. Genet.* **8**, 9–22
- Sparmann, A., and van Lohuizen, M. (2006) *Nat. Rev. Cancer* **6**, 846–856
- Tillib, S., Petruk, S., Sedkov, Y., Kuzin, A., Fujioaka, M., Goto, T., and Mazo, A. (1999) *Mol. Cell Biol.* **19**, 5189–5202
- Faucheux, M., Roignant, J. Y., Netter, S., Charollais, J., Antoniewski, C., and Theodore, L. (2003) *Mol. Cell Biol.* **23**, 1181–1195
- Gildea, J. J., Lopez, R., and Shearn, A. (2000) *Genetics* **156**, 645–663
- Mishra, R. K., Mihaly, J., Barges, S., Spierer, A., Karch, F., Hagstrom, K., Schweinsberg, S. E., and Schedl, P. (2001) *Mol. Cell Biol.* **21**, 1311–1318
- Canudas, S., Perez, S., Fanti, L., Pimpinelli, S., Singh, N., Hanes, S. D., Azorin, F., and Espinosa, M. L. (2005) *Nucleic Acids Res.* **33**, 4857–4864
- Nagel, A. C., Krejci, A., Tenin, G., Bravo-Patino, A., Bray, S., Maier, D., and Preiss, A. (2005) *Mol. Cell Biol.* **25**, 10433–10441
- Struffi, P., Corado, M., Kulkarni, M., and Arnosti, D. N. (2004) *Development* **131**, 2419–2429
- Chinnadurai, G. (2007) *Int. J. Biochem. Cell Biol.* **39**, 1593–1607
- Mannervik, M., and Levine, M. (1999) *Proc. Natl. Acad. Sci. U. S. A.* **96**, 6797–6801
- Ryu, J. R., and Arnosti, D. N. (2003) *Nucleic Acids Res.* **31**, 4654–4662
- Phippen, T. M., Sweigart, A. L., Moniwa, M., Krumm, A., Davie, J. R., and Parkhurst, S. M. (2000) *J. Biol. Chem.* **275**, 37628–37637
- Atchison, L., Ghias, A., Wilkinson, F., Bonini, N., and Atchison, M. L. (2003) *EMBO J.* **22**, 1347–1358
- Srinivasan, L., and Atchison, M. L. (2004) *Genes Dev.* **18**, 2596–2601
- Struffi, P., and Arnosti, D. N. (2005) *J. Biol. Chem.* **280**, 40757–40765
- Subramanian, T., and Chinnadurai, G. (2003) *FEBS Lett.* **540**, 255–258